Journal of Basic and Environmental Sciences, 6 (2019) 121-130

ISSN
Online: 2356-6388
Print: 2536-9202

Research paper Open Access

New Rout for Preparation of Nanosized-Metal Oxides and Their Analytical Application

M.E. Moustafa[1], M.I. Ayad[2], and E. A. Mohamed[1]*

[1]Faculty of science, Benha University, Benha, Egypt,
[2]Faculty of science, Menofia University, Shiben El-Kom, Egypt

Abstract

This paper deals with the synthesis and characterization of MgO, ZrO_2 and MgO–ZrO_2 nanosized oxides and explore their biological and antitoxic effects. The photocatalytic efficiencies for the degradation of organic pollutants (malachite green) and adsorption removal of inorganic pollutant (arsenic) from water samples are also discussed. The as-prepared nanooxides were characterized by thermogravimetric – differential thermal analysis (TGA– DTA), Fourier transform infrared spectroscopy (FTIR), powder X – ray diffraction (XRD) and high-resolution transmission electron microscope (HRTEM). XRD patterns revealed that the nanoparticles consist mainly of (cubic) while HRTEM images show that they consist of rectangular rode shapes with weak agglomeration with average size of 50-100 nm. The optimum conditions for the maximum removal of dye degradation was proposed by varying the experimental parameters like initial concentration, dose, pH and contact time.

Keyword: Nanosized simple and mixed metal oxides; photocatalytic degradation of malachite green.
Received; 15 Oct 2018, Revised form; 28 Dec. 2018, Accepted; 28 Dec. 2018, Available online 1 April 2019

1. Introduction

Nanomaterials are considered as next generation materials that have attracted recent attention due to their novel properties differing from those of the bulk materials [1]. Photocatalysis is a booming field of chemistry due to its numerous potential applications. Using light as an energy source to drive a reaction in a desired direction has resulted in chemistry, which is much more 'green'. Photocatalysis had been considered as an effective alternate for the purification of dye from waste water [2]. Among of these oxides, zirconium oxide and magnesium oxide possess high catalytic activity toward organic pollutants due to their high surface area, crystallinity, different morphologies and easily separation of electron hole pairs which are necessary for generating free radicals which decompose organic pollutants [3-4]. Nano-adsorbents of mixed oxides such as iron-cerium, iron–manganese, iron-zirconium, iron-titanium, iron chromium, cerium-manganese were successfully employed for water treatment. Therefore, this study focused on the preparation, characterization and photocatalytic activity of zirconium, magnesium and mixed zirconia –magnesia nanoparticles.

2. Experimental

All chemical used in the present work were of highest purity analytical grade (Aldrich or Merck) and were used without further purification. Bidistilled water was used all over the work. The synthesis of nanoparticles metal mixed was as follows:

2.1. Synthesis of zirconium oxide nanoparticle.

Zirconium oxide nanoparticles (Z_1–Z_4) were prepared via the following procedure:

i- 6 gm of zirconyloxychloride was dissolved in 20ml distilled water; solution (A).

ii- 5.75 gm of sodium lauryl sulfate was dissolved in 20ml distilled water; solution (B) then each of polyethelenglycol(PEG), (PEG)400, PEG1500, PEG 6000 and polyvinyl alcohol (PVA) was added separately to get solutions (B) for Z_1, Z_2, Z_3 and Z_4, respectively.

iii- Solution (B) was added drop by with vigorous stirring to solution (A). The mixtures were stirred for 1 h. and the precipitates formed were filtered, washed thoroughly using bidistilled water, air dried, thoroughly grounded in agate mortar and finally dried at 120^{o}C for two hours to obtain the metal organic acid precursors in the form of fine powder.

iv- The powder so obtained was annealed at 750^{o}C for six hours in muffle furnace to obtain the corresponding zirconium oxide nanoparticles.

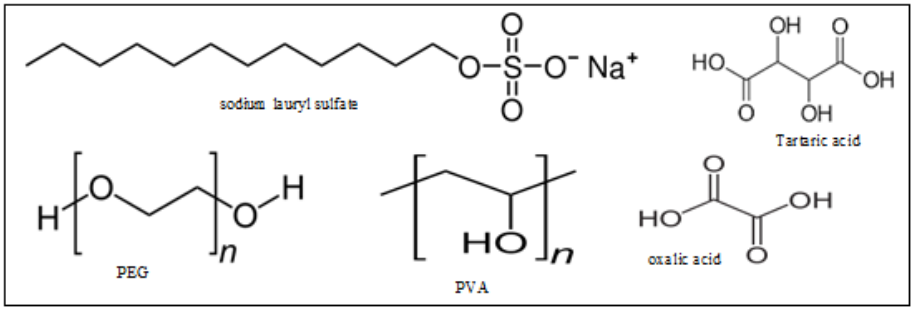

2.2. Synthesis of magnesium oxide nanoparticles.

For magnesium oxide nanoparticles (M_1 and M_2), 50 ml of each of 0.2 M of oxalic (M_1) and tartaric acid (M_2) was added drop by drop with constant stirring to a solution of 50 ml 0.1 M magnesium acetate (in 1: 2 M ratio). The mixtures were stirred for 1 h. and the precipitates formed were filtered, washed thoroughly using bidistilled water, air dried at 120ºC for two hours to obtain the metal organic acid precursors in the form of fine powder then ignited at 750°C for 5 hours to produce the corresponding magnesium oxide nanoparticles

2.3. Synthesis of zirconium- magnesium mixed oxide nanoparticles.

Magnesium-zirconium oxide nanoparticles (MZ) were prepared via co – precipitation of 50 ml 0.1 M magnesium acetate + 50 ml 0.1 M zirconyloxychloride) using drop by drop addition of 50 ml of 0.4 M oxalic (MZ), in 1: 2 M ratio. The mixture was stirred for 1 hour and the precipitate formed was filtered, washed thoroughly using bidistilled water, air dried then ignited at 750°C for 5 hours to produce the corresponding magnesium- zirconium mixed oxide nanoparticles.

2.4. Physical measurements

FT-IR spectra of both of the precipitated and ignited samples were recorded on a Nicolet iSio FT-IR spectrophotometer in the 4000– 400 cm^{-1} region using KBr disk technique (Chemistry department, Faculty of science, Benha University, Egypt). Electronic absorption spectra of the prepared nanooxides were recorded on a Jasco (V-530) UV–Vis spectrophotometer (Chemistry department, Faculty of Science, Benha University, Egypt). Thermo gravimetric analyses (TGA) for the organic precursors were recorded on Shimadzu TA-60 WS thermal analysis (Micro analytical unit, Menofia University, Shebin El – Kom, Egypt). X-ray powder diffraction (XRD) was recorded on a 18 kW diffractometer (Bruker; model D8 Advance) with monochromated Cu K_α radiation (λ) 1.54178 Å (Central metallurgical research institute, Helwan, Egypt). The HR-TEM images of some selected nanooxides were taken on a transmission electron microscope (JEOL; model 1200 EX) at an accelerator voltage of 220 kV (Egyptian Petroleum Research Institute, Cairo, Egypt). Arsenic ion content was measured by atomic absorption spectrophotometer (Szhimadzu AA7000) (Faculty of Agriculture, Benha University, Egypt).

2.5. Adsorption activity measurements

2.5.1. Arsenic removal from wastewater by nanosized oxides

The efficiency of some of the as-prepared oxide nanoparticles for the removal of As (V) from water samples was assessed. The effect of different parameters controlling the efficiency of removal process was studied. A stock solution of arsenate (10^3 μg/L) was prepared in double distilled water using disodium hydrogen arsenate heptahydrate ($Na_2HAsO_4 \cdot 7H_2O$). Further dilutions using double distilled water were made to prepare the solutions of different concentrations required at different level of experiments. The pH of the test solutions was adjusted using reagent grade dilute hydrochloric acid and sodium hydroxide (0.1M). InoLab 726 pH meter (Ser-No 09210173) was used to measure the pH of solutions.

All experiments were conducted in 50 mL polypropylene centrifuge tubes (Corning 430829). 100 mg of the nanoparticles were placed in the tubes, and then, the arsenic sample was added. The tubes were sealed and placed on a bench top orbital shaker table (Labline Orbit Shaker) set at 250 rpm. The samples were allowed to react with nanoparticles for a period of time between 5 and 120 min. After the set reaction time, the samples were centrifuged for 2 min to allow the nanoparticles to settle at the bottom of the tubes. The supernatant was then filtered using a syringe filter (Millipore 0.45 μm) and then collected in a beaker for arsenic analysis. Samples were acidified with nitric acid and analyzed for arsenic concentrations using atomic absorption spectra.

Investigated parameters:

- **Effect of contact time on the removal efficiency of metal ion:** Adsorption process was processed for different shaking time of 5–120 minutes. The other variables, i.e. initial concentration, dose, pH and temperature, were kept constant.
- **Effect of pH on the removal efficiency of metal ion:** Adsorption process was processed for different pH values of 2.0, 3.5, 5.5, and 7, at constant contact time, initial concentration, and temperature.
- **Effect of initial concentrations on the removal efficiency of metal ion:** Adsorption process was evaluated for different initial metal ion concentrations of 20, 50, 75, 100 and 120 ppm at constant pH values, constant contact time and temperature.

2.5.2. Photocatalytic degradation of malachite green (MG) dye

The photocatalytic degradation of 50 ppm malachite Green dye aqueous solution was performed using the smallest crystal sized zirconium oxide (Z_1), magnesium oxide (M_2) and mixed zrocnia – magnesia oxide (MZ) samples (prepared from PEG 400 tartaric acid and oxalic respectively). For a typical photocatalytic experiment, 100 mg of the nanooxide photocatalyst was added to 25 ml of 50 ppm aqueous dye solution which was kept in dark for 6 h to allow the system to reach an adsorption desorption equilibrium then 2 ml of 0.5 M hydrogen peroxide solution was added. The degradation process was investigated in a Pyrex beaker under the UV illumination using a 250 W xenon arc lamp (Thoshiba, SHLS-002) (λ = 365 nm). After recovering the catalyst by centrifugation, the light absorption of the clear solution was measured at 614 nm (λ_{max} for malachite green dye) at different time intervals using a UV–Vis spectrophotometer.

2.6. Antimicrobial Screening

The antibacterial activity of some selected nanoparticles toward four bacterial strains [two Gram – positive bacteria (*Streptococcus pyogenes* and *Staphylococcus epidermidis*) and two Gram – negative bacteria (*salmonella typhi* and *Escherichia coli)]* was measured by agar well diffusion method [5]. Standard drug; Ampicillin and DMSO solvent control were screened separately for their antibacterial activity. The tested compounds were dissolved in DMSO to get concentration of 100 µg/mL. A hot nutrient agar solution (20 ml) was poured into the sterilized petri dishes and allowed to attain room temperature. The seed layer medium was melted and cooled to ≈ 45ºC with gentle shaking. The previously grown subculture was added to the seed layer medium aseptically and mixed well. It was immediately raked into the petri dishes and allowed to attain room temperature. Then wells were made with the sterile cork porer and to these wells, 50 µl in concentration of 100 µgl/ml of the tested compound was added and the plates were allowed to cool for one hour to facilitate the diffusion. The plates were incubated at 37ºC for 24 hours. Antibacterial activity of the complexes was evaluated by measuring the diameter of zone of inhibition in mm. The medium with DMSO as solvent was used as a negative control whereas media with Ampicillin were screened separately for its standard antibacterial activity.

2.7. Antitumor activity assay.

In vitro anticancer activity evaluation of some selected nano particles was carried out against human cancer cell lines hepatocellular carcinoma (HePG-2) using MTT method at The Regional Center for Mycology & Biotechnology, Al – Azhar University, Cairo, Egypt. The viable cells yield was determined by a colorimetric method [6]. The relationship between sample concentrations and cell viability was plotted to calculate the IC_{50} values. The 50% inhibitory concentration (IC_{50}), the concentration required to cause toxic effects in 50% of intact cells, was estimated from graphic plots of the dose response curve for each conc. using Graphpad Prism software (San Diego, CA. USA) [7]

3. Results and discussion

Characterization of the as-prepared samples

3.1. Thermal analysis:

The thermogravimetric-differential thermal analysis was performed on the organic salt precursors before ignition at 750ºC and on the nanooxides obtained after ignition to follow their thermal decomposition to the final oxide forms. The TGA-DTA curves of selected sample is shown in Fig.(1a-b) and the data of thermal events are listed in Table (1). Also, the thermodynamic and kinetic parameters of the nanooxides were estimated from DTG curves by using piloyan and initial rate method [8,9] as shown in Fig. (2a-b) and data listed in Table (2) which showed that the reaction proceeding via first order reaction. Inspection of the data obtained showed that the organic salt precursors were thermally degraded through, more or less, four main steps as expected**.** The first step within the temperature range 23.34 – 180.04ºC represents the removal of physically adsorbed water molecules from the outer surface of the compound, the second step is due to the dehydration of crystallinity water and starting decomposition of organic precursors (this step is sometimes a composite of two steps) within the temperature range 232-494 ºC. The beginning of the thermal degradation of the anhydrous compounds took place within the third step e evolution of gases such as Cl& CO_2. Complete decomposition of the organic precursors occurred in the fourth step within the range 280 – 655.62ºC which led to the formation of the nanosized ZrO, MgO or Zr – MgO as final products.

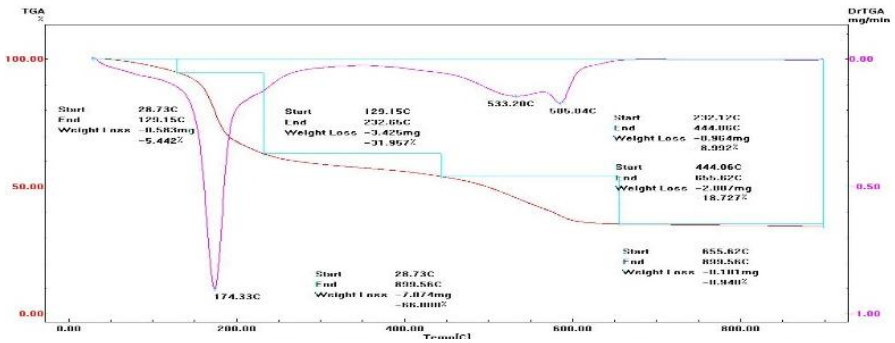

Fig. (1a): thermal analysis of precursor Z1 before ignition

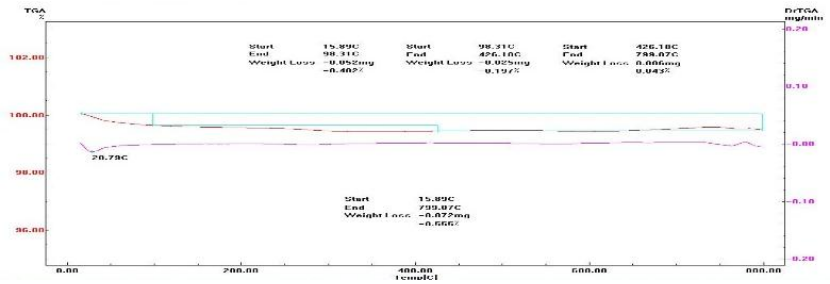

Fig. (1b): thermal analysis of precursor Z1 after ignition at 750ºC

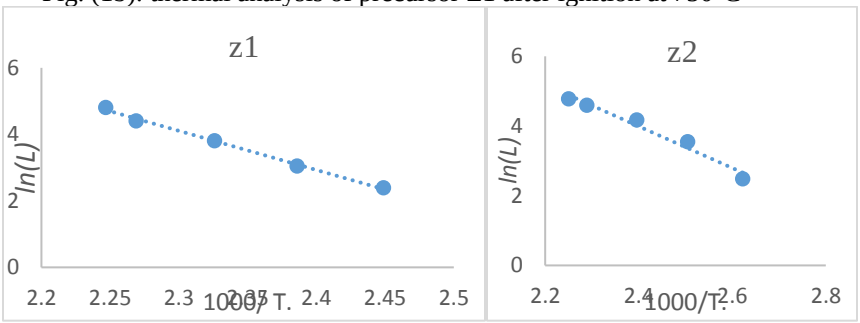

Fig(2a-b): Plots for the decomposition of $Z_1$and Z_2 by piloyan and initial rate using the data from the DTG curves.

Table (1): Thermogravimetric data for the polyethylene glycol (PEG) and organic acids precursors.

Compound	Temp.(ºC)	Wt. loss %	Assignment
Z_1	28.73-129.15	5.442%	-Removal of physically adsorbed $H_2O$and H_2O from PEG400.
	129.15- 444.06	40.94%	-Removal of water of crystallization &starting decomposition of sodium lauryl sulfate &removal of Cl_2 & or HCl gases and another organic residue.
	444.06 -655.62	18.72%	- Decomposition of anhydrous Zr-salt residue.
Z_2	23.34 -111.62	5.604%	-Removal of physically adsorbed H_2O.
	111.62 -280.54	41.435%	-Removal of water of crystallization& starting decomposition of sodium lauryl sulfate &removal of Cl_2 & or HCl gases.
	280.54 -616.18	19.410%	-Removal of other organic residues& Decomposition of anhydrous Zr-salt residue.
Z_3	23.41 -100.842	4.270%	-Removal of physically adsorbed H_2O.
	100.84 -262.98	48.792%	-Removal of water of crystallization &starting decomposition of sodium lauryl sulfate &removal of Cl_2 & or HCl gases and other organic residue.
	262.98-616.45	9.41%	-Decomposition of anhydrous Zr- salt residue.
Z_4	26.95 – 142.14	4.837%	-Removal of physically adsorbed H_2O.
	142.14 – 410.18	3.230%	-Removal of water of crystallization.
	410.18 – 677.04	10.388%	-Decomposition of anhydrous Zr-salt residue.
M_1	25.59 -180.04	7.78%	-Removal of physically adsorbed H_2O.
	180.04 - 412.21	21.538%	-Removal of water of crystallization.
	412.21 – 539.19	43.352%	-Decomposition of anhydrous Mg-oxalate and other Mg residue.
M_2	26.60 -246.01	23.548%	- Removal of physically adsorbed H_2O& water of crystallization
	246.01 – 371.81	24.987%	- Removal of co_2, OH &Decomposition of organic precursor.
	371.81 -494.93	30.348%	-Removal of Decomposition of anhydrous Mg-tartrate.and other Mg residue.
ZM	27.61 -165.64	16.748%	-Removal of physically adsorbed H_2O
	165.94- 268.18	8.593%	-Removal of water of crystallization.
	268.18– 568.77	36.6%	-Decomposition of anhydrous ZM residues

Table:(2): Kinetic parameters of the thermal decomposition of prepared nano-oxides and Fick's law.

compound	Temperature Range (°C)	DTG Peak (°C)	n	E_a/ KJ/mol	ΔH KJ/mol	n from Fick's law
	72 - 230	171	1.236	97.897	94.32	0.8987
Z_1	558 - 610	589	1.178	193.90	191.20	Non – fickian
	88 - 254	171	1.313	49.612	46.078	0.775
Z_2	520 - 690	243	0.78	55.31	52.54	Non – fickian
		581	0.849	149.25	146.20	
		651	1.028	165.33	162.92	
	102 - 232	176.5	.005	47.53	44.18	0.9897
Z_3	464 -624	580	0.73	90.53	86.95	Non – fickian
	20 – 120	41.5	1.78	10.69	7.32	0.5349
Z_4	450 - 578	509	1.18	94.4	91.06	Non – fickian
	15 – 69	44	1.2	54.59	51.86	
M_1	171 – 250	228	0.73	121.6	118.69	0.9622
	512 – 434	492	0.72	293.8	290.95	Non – fickian
	18 – 129	72.62	1.4	21.53	18.33	0.897
M_2	268 - 367	311	1.2	117.03	113.93	Non – fickian
	381 - 468	430	1.1	114.41	111.43	
	38 – 161	72	1.4	41.47	38.18	
MZ	173 – 236	209	1.1	103.9	101.62	1.09
	283 -440	324	1.7	94.05	90.48	Non – fickian

3.2. Fourier transform infrared spectra (FTIR)

The FTIR spectral data of the as-prepared samples are listed in Table (3). The spectra of the organic acid precursors show weak absorption bands within the wavenumber ranges 3373 - 3430 cm^{-1} and 1033 - 1176 cm^{-1} due to the stretching and bending vibrations of the trace water molecule, respectively. These two bands appeared within the ranges 2955 – 3430 cm^{-1} and 1032 – 1176 cm^{-1} as very weak bands in the spectra of the ignited samples. The strong bands within the range 1570 - 1677$cm^{-1}$are due to the stretching vibration of C=O group ($V_{C=O}$). These bands, more or less, disappeared in case of calcinated sample. The stretching vibration band of the S=O group of the lauryl sulfate appears at 1270 cm^{-1} in the uncalcinated species.

It is worthy to mention that there is a shift in the IR active mode, which is due to nano size grain. For a nano size grain, the atomic arrangement on the boundaries differ greatly from that of the bulk crystals, both in coordination number and bond lengths, showing some extent of disorder [10] Crystal symmetry is thus, degraded in nano size grains. The degradation in crystal symmetry results in the shifting of the IR active mode [11].

Table (3): IR frequencies (cm^{-1}) of some important groups for organic acid precursors and the nanooxide.

Compound	IR frequency (cm^{-1})					
	ν_{OH}	δ_{OH}	$V_{C=O}$	ν_{C-O}	$V_{S=O}$	M-O
Zr –laur. SO_4-PEG (Z_1)	3425 .52	1115.64	1624	885	1270	---
	$3430_{v.w}$	1085	---	---	---	553
Zr- laur. SO_4-PEG 1600 (Z_2)	3430.71	1176.47	1691	893.54		---
	$3110_{v.w}$	1152.45	---	---	---	544
Zr- laur. SO_4-PEG 6000(Z_3)	$3404.33_{br.}$	1084.14	1570	870.23		---
	$3052_{v.w}$	1171.25	---		---	570
Zr- laur. SO_4—PVA(Z_4)	3428	1032.77	1677	913.15		---
	$3362_{br.}$	1136.70	---	---	---	583
Mg- oxalate (M_1)	$3389_{br.}$	1128.96	1637	829.92	---	---
	2955_{vw}	1166.68	---	---	---	541
Mg- tartarate (M_2)	3408_{br}	1090.45	1617	832.88	---	---
	$2979_{v.w}$	1135.71	---	---	---	542
Zr-Mg precursor (MZ)	3373_{br}	1033.78	1617	924.83		---
	3381	1095.12	---	---	---	522

br. broad v.w very weak

3.3. X-ray diffraction:

Representative X-ray diffraction patterns of the nano sized zirconium, magnesium and their mixed oxides, prepared by co-precipitation method, are shown in (Fig.'s; 3 and 4). The XRD sharp lines reveal that the nanoparticles of the oxides are crystalline. with mean grain size 14.35, 20.173, 30.19, 22.138 and 14.6 nm f for Z_1 ,Z_2, Z_3 ,M_2 and MZ respectively The relative crystalline sizes are determined from the XRD lines broadening using the Scherrer equation [12, 13] . From the data nanosized metal oxides have different crystallite size, this is may be ascribed to the different types of organic precursor.

$$D = \frac{k\lambda}{\beta_{hkl}} / cos\theta_{hkl}$$

In the XRD pattern, three prominent diffraction peaks were observed at 2Θ values correspond to (111), (200) and (220) Bragg's reflections of the face – centered cubic (fcc) structure. The phase purity of all the samples was established by comparison of the X-ray diffraction patterns with JCPDS international data value.

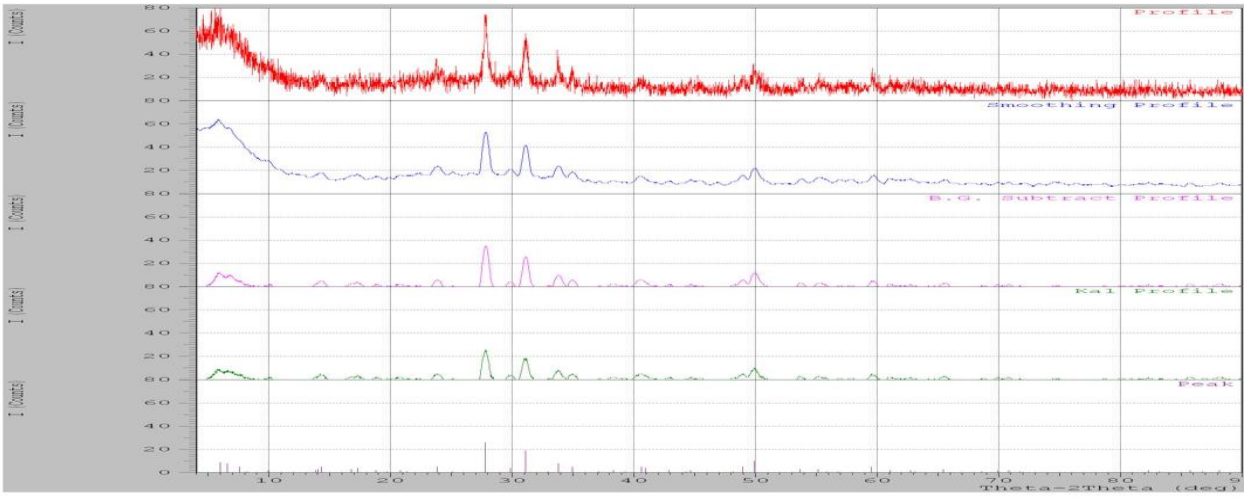

Fig. (3): XRD of the sample zirconium precursors [(Zr-lauryl sulfate with PEG400)[Z_1]]

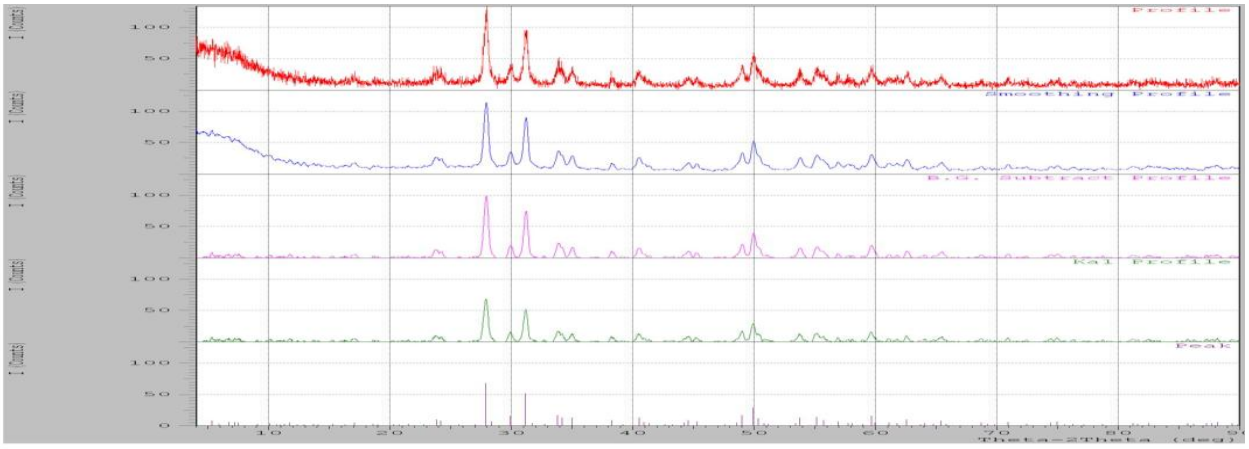

Fig. (4): XRD of the sample zirconium precursors [(Zr-lauryl sulfate with PEG1500)[Z_2]

3.4. High Resolution Transmission Electron Microscopy (HRTEM):

The morphologies and microstructures of some selected as-prepared samples calcined at 750°C for 6 hours were investigated with HRTEM. The TEM images of representative samples are shown in (Fig. 5a-b) It can be seen from the graphs that magnesium nanoparticles have narrow size distribution and are rectangular rode shapes with weak agglomeration. The average particle sizes ranged from 50 - 100 nm. All images are appeared to be high crystallinity.

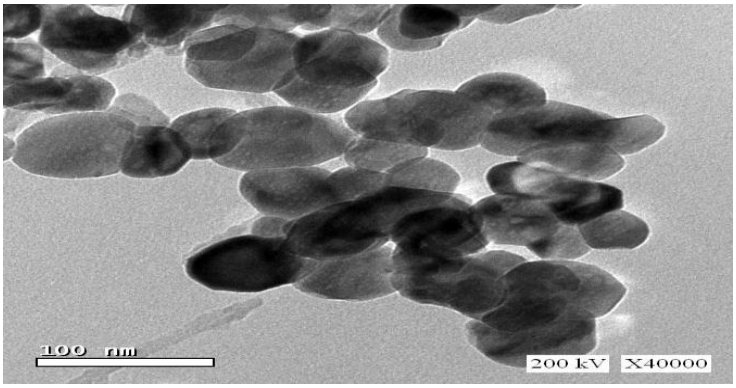

Fig. (5-a): HRTEM of the sample the sample the sample zirconium precursors [(Zr-lauryl sulfate with PEG1500)[Z_2]

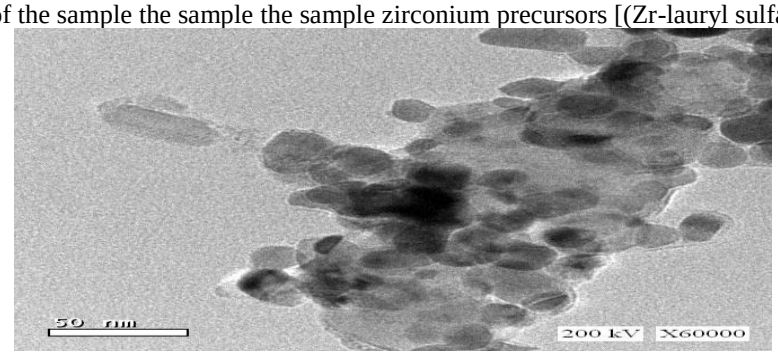

Fig. (5-b): HRTEM of the sample the sample the magnesium - zirconium precursors [(Mg- Zr oxalate) [MZ].

Adsorption activity measurements

Arsenic removal from wastewater by nanosized oxides

The efficiency of the nanooxide (sample Z_1) for the removal of As (V) from water samples was assessed. The effect of different parameters controlling the efficiency of removal process was studied.

Adsorption studies

The optimisation of the adsorption was achieved by varying various experimental variables. The optimised adsorption parameters were concentration of arsenate, contact time, pH, dose and temperature. The results were expressed as the percent removal of the adsorbent on metal ion, which is defined as

$$\% \text{ Removal} = [(C_o - C_1) / C_o] \times 100,$$

Where C_o and C_1 are the initial and equilibrium concentrations of metal ion solution (mg/l), respectively.

1- Effect of contact time

Time effect is very important parameter. The other variables, i.e. initial concentration, dose, pH and temperature, were kept constant. The results are given in Fig.(6) These results indicate that removal efficiency increased with an increase in contact time before equilibrium is reached.

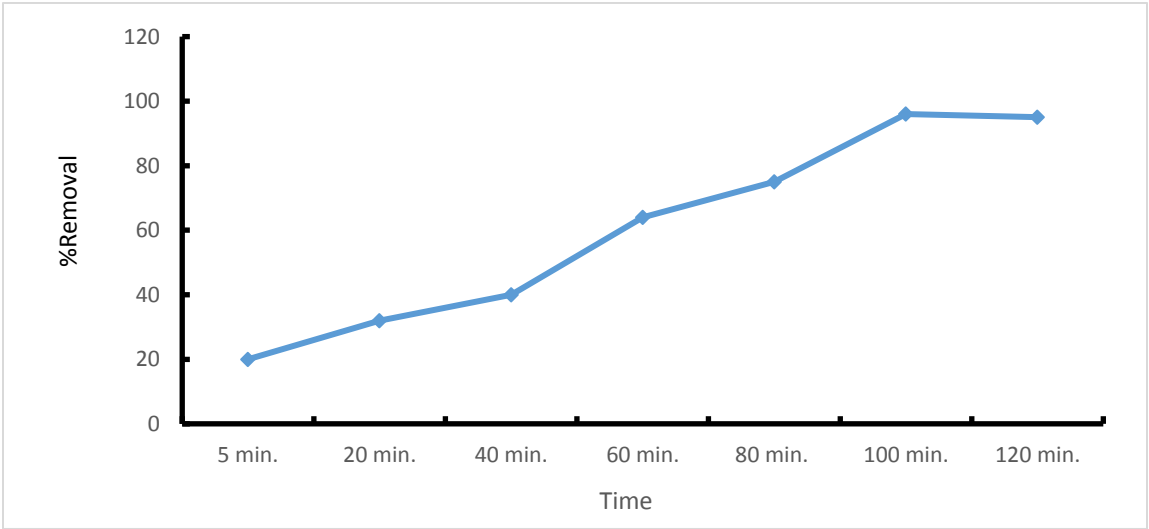

Fig (6): Effect of contact time on the percentage of removal of As(V) using Z_1 as sorbent.

2-Effect of initial concentration:

Results showed that adsorption is highly dependent on initial concentration of adsorbant. That is because the fact that at lower concentration, the ratio of the initial number of metal ion to the available surface area is low subsequently the fractional adsorption becomes independent of initial concentration. However, at high concentration the available sites of adsorption become fewer and hence the percentage removal of metal ion is dependent upon initial concentration. Equilibrium have established at 100 ppm.

3- Effect of pH

pH is one of the most important parameters controlling the metal ion adsorption results are given in Fig. (7) showed that the adsorptive removal of the metal ions under study from aqueous solutions at different pH values of the solution was maximum at pH between 7.00 – 8.00.

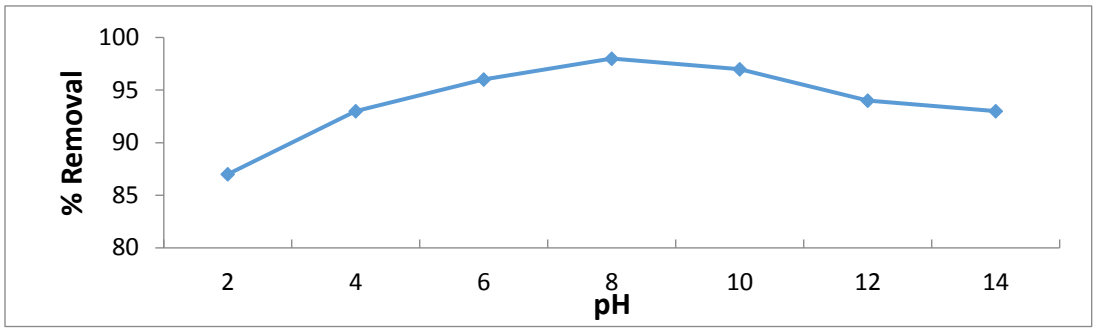

Fig. (7): Effect of pH on the percentage of removal of As(V) using Z_1 as sorbent.

Photocatalytic activity

The photodegradation efficiency of selected zirconium oxide nano-particle (sample Z_1; prepared from sodium lauryl sulfate and polyethelenglycol (PEG) 400 as organic precursors was tested using malachite green (MG) as model. At periodic intervals of time, aliquots of the sample were withdrawn, and the absorption spectra were measured at 618 nm. Clearly, the absorbance decreases and the photodegradation efficiency increases (reaching a plateau) as a function of time as shown in Fig (8).

A scan of the absorption spectra of MG shows two maximum bands (A; at 617.9 nm) and (B; at 461 nm) due to the absorption of undegraded and degraded species, respectively. The effect of photocatalytic degradation of MG led to the decrease in absorbance of band (A) and the increase in absorbance of band (B) with time. The mechanism of degradation is as follows:

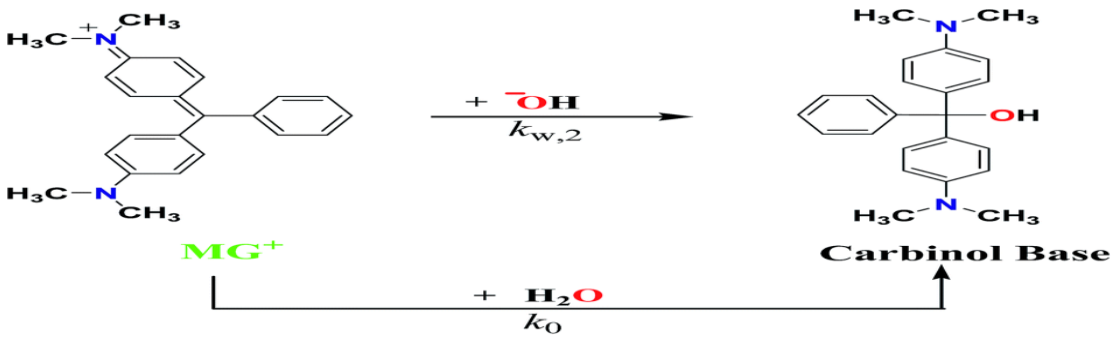

The results showed that the maximum percent of degradation of MG dye after 210 min was 69% in case of UV only ,83% after210 min in case of UV+ H_2O_2 while, it reached to 95.4% after 180 in the case of UV+ Z_1 nanoparticle as catalyst While,98% degradation after 180 using of (UV radiation +H_2O_2 as catalyst + Z_1 nanoparticle as catalyst). indicating the very high efficiency of Z_1 as photocatalyst for MG.

-

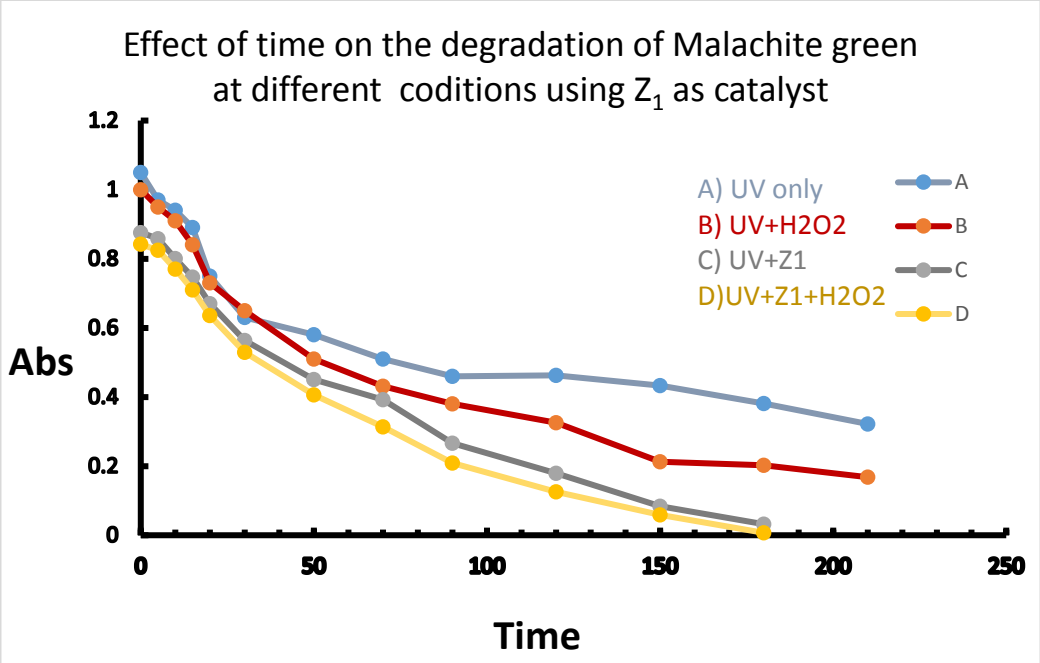

Fig. (8): Effect of time on the absorption spectra and degradation efficiency of MG dye in presence of nanoparticle z_1 as catalyst

Antimicrobial activity

The antibacterial results of the nanosized metal oxides (*c.f.* Table 4) suggest that the nanooxides show high activity against the tested organisms compared to Ampicillin taken as a standard drug. Although there is no general trend concerning the antimicrobial effect of the tested nanoparticles, but the activity of Magnesium- Zirconium mixed nanooxide showed higher activity than other tested nanooxide.

Table (4) Inhibition zone diameter (mm) of the oxide nanoparticles against various microorganisms

Organism	Strept. Pyog.			Staph. Epid.			salmonella typhi s			Escherichia coli		
Conc. (µg/mL)	5	10	20	5	10	20	5	10	20	5	10	20
Ampicillin	15	18	20	15	17	25	13	16	23	15	18	25
Z_1	15	18	21	12	17	22	13	17	24	16	18	23
Z_2	12	16	19	12	16	22	14	16	20	14	17	22
M_1	13	15	18	14	16	19	12	14	18	11	14	16
M_2	12	15	16	11	15	17	11	13	17	13	16	18
MZ	14	17	22	13	18	23	14	18	25	17	19	23

Antitumor activity

Inspection of the cytotoxic data, it is found that Magnesium oxide M_2 (prepared from tartaric acid as organic precursors) is, in general, more effective than those of zirconium oxides Z_1 and Z_4 (prepared from sodium lauryl sulfate and polyethelenglycol (PEG)400 and polyvinyl alcohol (PVA) as organic precursors, respectively) and MZ the mixed nanooxide (prepared from oxalic acid). Magnesium oxide M_1 prepared from oxalic acid and, on the other hand, has the lowest activity toward the examined cell line having a high value of IC_{50} (106.0 µg/mL). So, the nanosized metal oxides under study are considered to have weak activity with IC_{50} values 12.9 – 106 µg/mL [14]. the lethal concentrations (IC_{50}) values are listed in Table (5).

Table (5): Lethal concentration (IC_{50}) of the nanosized oxides under study.

Oxide	IC_{50} (µg/ml)
Vinblastine	4.6
Z_1	22.5
Z_4	53.8
M_1	106.0
M_2	12.9
MZ	44.3

References

[1] E. Roduner "Size matters: why nanomaterials are different", Chem. Soci. Rev., (2006).

[2] R.Ameta , M. S.Solanki , S.Benjamin, S. C.Ameta ; "Advanced Oxidation Processes for Waste Water Treatment", Emerging Green Chem. Tech. (2018)135-175.

[3] L. Renuka, K.S. Anantharaju, S.C. Sharma, H.P. Nagaswarupa, S.C. Prashantha, H. Nagabhushana and Y.S. Vidya "Hollow microspheres Mg-doped ZrO_2 nanoparticles: green assisted synthesis and applications in photocatalysis and photoluminescence", J. Alloys Compd., 672 (2016) 609–622.

[4] A.A. Ashkarran, S.A.A. Afshar, S.M. Aghigh and K. Mona, "Photocatalytic activity of ZrO_2 nanoparticles prepared by electrical arc discharge method in water", Polyhedron, 29 (2010) 1370–1374.

[5] A. W. Bauer, M.D. W. M. M. Kirby, J. C. Sherris, M. Turck "Antibiotic susceptibility testing by a standardized single disk method" , Am. J. Clin Pathol, 45 ,(1966) 493–496.

[6] Mosmann, T.; "Rapid colorimetric assay for cellular growth and survival: application to proliferation and cytotoxicity assays" J. Immunol. Methods, 65 (1983) 55-63.

[7] S. M Gomha, S.M Riyadh, El-M.A. Mahmmoud. and M.M. Elaasser "Synthesis and Anticancer Activities of Thiazoles, 1,3-Thiazines, and Thiazolidine Using Chitosan-Grafted-Poly(vinylpyridine) as Basic Catalyst. Heterocycles", Int. j.for rev. &com. hetero. chem., 91 (2015)1227-1243.

[8] Y. Kirsh, S. Yariv, S. Shoval, Kinetic analysis of MgCl2.6H2O by DTA and DTG, J. Therm. Anal. Calorim. 32 (1987) 393e408.

[9] G.O. Piloyan, I.D. Ryabchikov, O.S. Novikova, Determination of activation energies of chemical reactions by differential thermal analysis, Nature 212 (1966) 1229.

[10] A. K. Adak and A. Pathak;"Synthesis, Characterization and Physicochemical Properties of Nanosized Zn/Mn oxides system", British Ceramic Transaction, 98 (4), (1999) 200-203.

[11] Pirogova, C. N., N. M. Panish, R. I. Karosteleva and Y. V. Voronin; "Synthesis, Characterization and Dye Adsorption of Ilmentite Nanoparticles', Russian Chem. Bull., 46 (1994)1634-1636.

[12] P. Scherrer, Göttinger Nachrichten Gesell., 2 (1918) 98.

[13] A. Patterson, "The Scherrer Formula for X-Ray Particle Size Determination", Phys. Rev., 56 (10) (1939) 978–982.

[14] W. T. Shier; Mammalian Cell Culture on 5 a day: a Laboratory Manual of Low Cost Methods. University of the Philippines, Los Banos, (1991).